

# B-Flow Sonography vs. Color Doppler Sonography for the Assessment of Vascularity in Pediatric Kidney Transplantation

## B-Flow-Sonografie im Vergleich mit Color-Doppler-Sonografie zur Evaluation der Gefäßversorgung transplantierte Nieren im Kindesalter

### Authors

Elena Dammann<sup>1</sup>, Michael Groth<sup>2</sup>, Raphael-Sebastian Schild<sup>3</sup>, Anja Lemke<sup>3</sup>, Jun Oh<sup>3</sup>, Gerhard Adam<sup>1</sup>, Jochen Herrmann<sup>2</sup>

### Affiliations

- 1 Department of Diagnostic and Interventional Radiology and Nuclear Medicine, University Medical Center Hamburg-Eppendorf, Hamburg, Germany
- 2 Section of Pediatric Radiology, Department of Diagnostic and Interventional Radiology and Nuclear Medicine, University Medical Center Hamburg-Eppendorf, Hamburg, Germany
- 3 Department of Pediatric Nephrology, University Medical Center Hamburg-Eppendorf, Hamburg, Germany

### Key words

ultrasonography, doppler, color, kidney transplantation, child

received 27.06.2019

accepted 20.04.2020

### Bibliography

DOI <https://doi.org/10.1055/a-1167-8317>

Published online: 2020

Fortschr Röntgenstr

© Georg Thieme Verlag KG, Stuttgart · New York

ISSN 1438-9029

### Correspondence

PD Dr. med. Jochen Herrmann

Pädiatrische Radiologie, Abteilung für Diagnostische und Interventionelle Radiologie und Nuklearmedizin, Universitätsklinikum Hamburg-Eppendorf, Martinistraße 52, 20246 Hamburg, Germany  
j.herrmann@uke.de

### ZUSAMMENFASSUNG

**Ziel** Die Beurteilung der Gefäßversorgung transplantierte Nieren im Kindesalter mittels B-Flow-Sonografie (BFS) im Vergleich zur Color-Doppler-Sonografie (CDS).

**Patienten und Methoden** Alle Kinder nach Nierentransplantation, die im Zeitraum von Januar 2013 bis Januar 2016 in unserer Klinik eine protokollbasierte Ultraschalluntersuchung in BFS- und CDS-Technik mit identischen Grundeinstellungen erhielten (Loqiq 9, GE Medical Systems, Milwaukee, WI, USA), wurden retrospektiv evaluiert (n = 40). Die erhaltenen Bilddaten wurden visuell klassifiziert: (I.) Darstellung des gesamten

renalen Gefäßbaums (Grad 1 – interlobäre, arcuatae und interlobuläre Gefäße abgrenzbar; Grad 2 – interlobäre und kortikale Gefäße abgrenzbar, nicht arcuatae von interlobulären Gefäßen abgrenzbar; Grad 3 – nur interlobäre Gefäße abgrenzbar; Grad 4 – insuffiziente Abgrenzbarkeit), (II.) Dichte der Kortexgefäße im ventralen, lateralen und dorsalen Nierenanteil, (III.) geringster Gefäß-Kapsel-Abstand und (IV.) maximale Anzahl von Kortexgefäßen. Der statistische Vergleich erfolgte mittels exaktem Fisher-Test und gepaartem T-Test.

**Ergebnisse** Unter Verwendung eines Sektorschallkopfes (C1–6) zeigte BFS im Vergleich mit CDS eine vollständigere Darstellung des renalen Gefäßbaums ( $p < 0,001$ ) mit einem geringeren Gefäß-Kapsel-Abstand ( $p < 0,001$ ) und einer höheren maximalen Gefäßdichte im ventralen Kortex ( $p < 0,001$ ) mit einer höheren max. Anzahl von Gefäßen ( $p = 0,01$ ). Im dorsalen und lateralen Transplantatanteil war die nachweisbare Gefäßdichte niedriger mit BFS als mit CDS (jeweils  $p < 0,001$ ). Unter Verwendung eines hochauflösenden Linear-schallkopfes (ML 6–15) konnte kein Unterschied zwischen BFS und CDS nachgewiesen werden.

**Schlussfolgerung** Eine verbesserte Darstellung des Vaskularisationsgrades von Nierentransplantaten im Kindesalter kann erreicht werden, indem BFS zum Standardprotokoll hinzugefügt wird. Die BFS zeigt insbesondere Vorteile in der Erfassung des renalen Gefäßbaums und der Charakterisierung der schallkopfnahen Kortexgefäße unter Verwendung eines Konvexschallkopfes

### Kernaussagen:

- BFS verbessert die Darstellung des Gefäßbaums und der schallkopfnahen Kortexregion in Nierentransplantaten.
- Im dorsolateralen Kortex ist die Gefäßdarstellung mit CDS aufgrund besserer Penetration günstiger.
- Die Ergänzung eines Standardprotokolls mit BFS erlaubt ein qualitativ verbessertes Transplantatmonitoring.

### ABSTRACT

**Objective** To compare B-flow sonography (BFS) with color Doppler sonography (CDS) for imaging of kidney transplant vascularization in children.

**Patients and Methods** All children receiving a kidney transplantation who underwent a protocol-based ultrasound

examination (Loqiq 9, GE Medical Systems, Milwaukee, WI, USA) using the BFS and CDS technique with equal settings and probe position between January 2013 and January 2016 were retrospectively assessed ( $n=40$ ). The obtained datasets were visually graded according to the following criteria: (I) delineation of the renal vascular tree (Grade 1 – clear demarcation of interlobar, together with arcuate and interlobular vessels; Grade 2 – clear demarcation of interlobar and cortical vessels, but no distinction of interlobular from arcuate vessels; Grade 3 – only clear demarcation of interlobar vessels, Grade 4 – insufficient demarcation) (II) delineation of cortical vessel density in ventral, lateral, and dorsal part of the transplant, (III) smallest vessel-capsule distance, and (IV) maximum cortical vessel count. Comparison between methods was performed using Fisher's exact and paired sample t-tests.

**Results** Applying a curved transducer (C1–6), BFS showed superior delineation of the renal vascular tree ( $p<0.001$ ), a lower vessel-capsule distance ( $p<0.001$ ), a higher cortical vessel count ( $p<0.001$ ), and a higher cortical vessel density in the superficial cortex ( $p=0.01$ ) than CDS. In the dorsal and lateral aspects of the transplant, cortical vessel density was

lower with BFS (both  $p<0.001$ ). Using a linear high-resolution transducer (ML 6–15), no significant differences between the methods were found.

**Conclusion** Improved imaging of kidney transplant vascularization can be achieved in children by adding BFS to a standard protocol. The BFS technique is especially beneficial for overall assessment of the renal vascular tree together with the extent of cortical vascularization on curved array images.

#### Key points:

- Depiction of vascular tree and ventral cortical vessels is improved by BFS.
- The dorso-lateral cortex was better represented with CDS because of higher penetration.
- Additional monitoring with BFS improves the monitoring of transplant viability.

#### Citation Format

- Dammann E, Groth M, Schild R et al. B-Flow Sonography vs. Color Doppler Sonography for the Assessment of Vascularity in Pediatric Kidney Transplantation. *Fortschr Röntgenstr* 2020; DOI 10.1055/a-1167-8317

## Introduction

Ultrasound is the method of choice for noninvasive monitoring of kidney transplants at the bedside [1, 2]. Standard protocols assess parenchymal integrity based on B-mode and flow imaging techniques. For vascularity assessment color Doppler sonography (CDS) including duplex ultrasound is generally the modality of choice. In adults, contrast-enhanced ultrasound (CEUS) has become increasingly relevant for a more specific diagnosis of allograft dysfunction [3]. Changes in renal vascularization and flow have been described in rejection, infection, urinary retention, and drug toxicity [4, 5].

Imaging of renal transplant vascularization with CDS is widely used because of the good signal-to-noise ratio and good penetration into deeper structures. However, known limitations of the method are the relatively low spatial and temporal resolution, aliasing effects with high-amplitude flow, angle dependency, and blurring artifacts [1, 4, 6–9]. Among alternatives, B-flow sonography (BFS) is a relatively new non-Doppler-based technique for the direct visualization of blood flow and was introduced in 2000 [10]. So far, BFS is available on the ultrasound platform of one manufacturer. The technique is based on the subtraction of received amplitudes of grayscale ultrasound resulting in angiography-like overlap free flow images with very high spatial and temporal resolution [11].

BFS was initially introduced for linear transducers and is now applicable for lower frequency convex probes, also allowing the evaluation of deeper structures such as abdominal organs. Side-by-side comparison with CDS showed that BFS is especially useful in areas with simultaneous low and high blood flow and for the detection of small vessels [12]. Preliminary studies have been

published in adult patients with carotid artery stenosis or ovarian torsion, and regarding the evaluation of vascularization in transplanted livers and kidneys [13–16]. Pediatric studies using BFS were reported for fetal congenital cardiopathies, femoral artery stenosis before catheterization in infants and anatomy of basal cerebral arteries in newborns [17–19]. The aim of this study was to compare BFS with CDS for the assessment of kidney transplant vascularization in children.

## Patients and Methods

### Patients

The study was approved by the institutional review board with a waiver of informed consent. All pediatric patients with kidney transplantation and who received a protocol ultrasound examination as part of their routine follow-up at our institution by the same single sonographer with corresponding CDS and BFS images between January 2013 and January 2016 were retrospectively assessed. If multiple examinations were available during this period, the most recent one was chosen. Of 47 consecutive cases performed during this period, 7 cases had to be excluded because of incomplete documentation or artifacts attributable to non-compliance. In total, 40 patients were included in this study (mean age  $11 \pm 4$  years, range 1–18 years; 24 male, 16 female). The mean interval between kidney transplantation and the ultrasound examination was  $1664 \pm 1420$  days (range 1–4820 days). Clinical data and laboratory findings of the patients were extracted from the patient record and are summarized in ► **Table 1**.

▶ **Table 1** Clinical patient data.

▶ **Tab. 1** Klinische Patientendaten.

patient	patient				current medication			current laboratory parameters			
	age (y)	BMI	days after TX	TX type	diagnosis leading to NTX	antihypertensives	immuno-suppressants	eGFR	urea (mg/dl)	creatinine (mg/dl)	cystatin C (mg/l)
1 m	17	19.7	2368	cad	1	1, 3, 4	1, 2, 4	53.89	15	1.25	1.08
2 m	4	17.1	793	cad	1	1, 3, 4	2, 4, 5	82.26	29	0.49	1.06
3 w	8	19.4	390	cad	1	3	1, 2, 4	131.95	13	0.4	1.22
4 w	8	16.6	897	cad	14	1, 3, 4	1.2	112.89	20	0.48	1.51
5 m	17	23.6	387	liv	16	1.3	1, 2, 4	31.19	34	2.25	n.a.
6 m	17	19.8	3301	cad	11	n.a.	n.a.	7.47	49	8.86	7.1
7 w	4	27.3	555	liv	4	1, 3, 4	1, 2, 4	123	n.a.	n.a.	0.77
8 w	17	18.5	4816	liv	15	1	1, 4, 7	57.49	29	1.14	n.a.
9 w	10	23.1	414	n.a.	1	1.3	1, 2, 4	68.56	19	0.95	1.22
10 m	2	15.3	445	liv	16	3	1.6	23.28	39	1.49	2.4
11 w	6	16.5	201	cad	4		1.6	110.48	20	0.4	0.69
12 w	12	23.2	2018	cad	1		1.2	54.23	22	1.07	1.03
13 m	10	14.7	2385	cad	9	1.4	1, 1, 2	51.81	20	1.1	n.a.
14 m	8	17.7	407	liv	16	3	1, 2, 4	90.11	14	0.55	0.99
15 m	4	16.3	1221	cad	1		5.2	49.79	39	0.9	1.6
16 w	11	15.5	2695	cad	8		1.2	62.74	31	1.04	1.34
17 w	12	17	3589	cad	4		1, 4, 7, 7	54.38	31	1.2	1.33
18 w	17	18	1728	cad	4	1.3	1, 2, 4	46.36	24	1.47	1.48
19 m	9	18.2	790	cad	14	1, 3, 4, 5	1, 2, 4	35.12	20	1.43	1.78
20 m	11	17.6	779	liv	8	3	1, 4, 7	37.4	51	1.59	1.64
21 m	1	14.8	449	cad	9	1, 3, 4, 5	2, 4, 5	20.1	47	3.4	2.53
22 m	9	17.5	2778	n.a.	12	1, 3.	1, 4, 7	33.31	39	1.55	1.83
23 m	14	17.8	1	n.a.	12	n.a.	n.a.	8.06	85	8.97	n.a.
24 m	10	16.3	1971	cad	16	3.4	1, 1, 6	43	n.a.	n.a.	1.56
25 w	14	20.3	135	cad	14	1, 3, 4, 5, 6, 8	1, 2, 4	45.4	31	1.46	1.24
26 m	13	21.2	3706	cad	1		1.7	61.43	23	1.03	1.28
27 m	9	17.5	356	liv	4	1.3	1.6	49.71	20	1.11	1.34

► Table 1 (Continuation)

patient	current medication				current laboratory parameters						
	age (y)	BMI	days after TX	TX type	diagnosis leading to NTX	antihypertensives	immunosuppressants	eGFR	urea (mg/dl)	creatinine (mg/dl)	cystatin C (mg/l)
28 m	10	15.4	90	cad	1	0	2, 4, 5	107.38	15	0.5	n. a.
29 w	16	27.1	2079	liv	1	1.3	1.7	99.12	10	0.67	0.73
30 m	15	20.6	2014	cad	1		1.6	50.98	24	1.4	1.42
31 w	12	19.3	2707	cad	7	3.4	2.5	59.53	21	1.11	1.29
32 w	16	20.2	2372	liv	1	1	1.3	74.25	16	0.9	0.73
33 m	18	20.7	4820	cad	4		2.5	38.9	n. a.	n. a.	n. a.
34 m	15	17.3	4293	cad	9	5, 6, 7	3, 4, 6	19.84	55	3.33	2.9
35 m	1	17.1	14	cad	12	n. a.	n. a.	6.23	85	4.97	n. a.
36 w	17	23.7	3234	cad	4	4	1.2	61.71	17	1.02	n. a.
37 m	7	14.7	2204	liv	7		5.7	32.24	28	1.5	1.4
38 w	15	20.4	2709	cad	4	1, 3, 4	1	17.09	43	3.48	n. a.
39 m	15	15.7	454	cad	16	2, 3, 4	1, 3, 4	47.52	20	1.46	0.92
40 m	7	14	10	n. a.	n. a.	n. a.	n. a.	n. a.	n. a.	n. a.	n. a.

y = years, BMI = body mass index, TX = transplantation, NTX = kidney transplantation, cad = cadaveric, liv = living, diagnosis leading to NTX: 1 = polycystic kidney disease; 2 = glomerulonephritis; 3 = hydronephrosis; 4 = kidney dysplasia; 5 = perinatal asphyxia; 6 = reflux nephropathy; 7 = Denys-Drash syndrome; 8 = hemolytic-uremic syndrome; 9 = CAKUT (congenital anomalies of the kidney and urinary tract); 10 = obstructive uropathy; 11 = prune belly syndrome; 12 = oxalosis; 13 = cystinosis; 14 = nephrotic syndrome; 15 = uro-anogenital malformation; 16 = posterior urethral valve, antihypertensives: 1 = Delix (ramipril + hydrochlorothiazide); 2 = Enalapril; 3 = Amlodipine; 4 = Beloc-Zok (metoprolol succinate + hydrochlorothiazide); 5 = Dihydralazine, immunosuppressants: 1 = tacrolimus; 2 = mycophenolate mofetil; 3 = mycophenolate; 4 = prednisolone, eGFR = estimated glomerular filtration rate calculated as in KDIGO 2012 Clinical Practice Guideline for the Evaluation and Management of Chronic Kidney Disease, n. a. = not available. Age (y) = Age (in Jahren); BMI = Body-Mass-Index; TX = Transplantation; NTX = Nierentransplantation; Days after NTX = Tage nach NTX; TX-type = TX-Art; cad = postmortem; liv = lebend; Diagnose, die zu einer NTX geführt hat: 1 = polyzystische Nierenerkrankung; 2 = Glomerulonephritis; 3 = Hydronephrose; 4 = Nierendysplasie; 5 = perinatale Asphyxie; 6 = Refluxnephropathie; 7 = Denys-Drash-Syndrom; 8 = hämolytisch-urämisches Syndrom; 9 = CAKUT (Congenital anomalies of the kidney and urinary tract); 10 = obstruktive Uropathie; 11 = Prune-Belly-Syndrom; 12 = Oxalose; 13 = Zystinose; 14 = nephrotisches Syndrom; 15 = uro-anogenitale Fehlbildung; 16 = posterior urethral valve; current medication = Medikation zum Zeitpunkt der Evaluation; Antihypertensiva: 1 = Delix (Ramipril + Hydrochlorothiazid); 2 = Enalapril; 3 = Amlodipin; 4 = Beloc-Zok (Metoprololsuccinat + Hydrochlorothiazid); 5 = Dihydralazin; Immunsuppressiva: 1 = Tacrolimus; 2 = Mycophenolat-Mofetil; 3 = Mycophenolat; 4 = Prednisolon; current laboratory parameters = Laborparameter zum Zeitpunkt der Untersuchung; eGFR = geschätzte glomeruläre Filtrationsrate, berechnet gemäß KDIGO 2012 Clinical Practice Guideline for the Evaluation and Management of Chronic Kidney Disease; n. a. = nicht verfügbar.

## Ultrasound monitoring

Image optimization including the CDS, power Doppler and BFS techniques was performed in a preliminary series of patients not included in this study. Power Doppler showed equivalent sensitivity regarding vessel delineation but more movement artifacts than CDS. To reduce examination time, power Doppler was consequently excluded from the final ultrasound protocol for pediatric patients with kidney transplantation. All examinations were performed by a single pediatric radiologist with 12 years of renal transplant ultrasound experience, using a commercial scanner (Logiq E9, GE Medical Systems, Milwaukee, WI, USA) with a curved transducer (C1–6) and a linear, high-resolution transducer (ML6–15). The standard technical settings for the C1–6 transducer were – frame rate (FR) 5, pulse repetition frequency (PRF) 1.4, mechanical index (MI) 1.2, thermal index in soft tissue (TIs) 1.0 for CDS and – FR 16, pulse repetition interval (PRI) 12, MI 1.2, TIs 1.1 for BFS. A high detection speckle reduction imaging (SRI HD) strength of 2 (ranging from 0–4) was used. The setting for the CrossXBeam technique was low, the CrossXBeam-type mean. The standard settings for the ML6–15 transducer were – FR 11, PRF 1.5, MI 0.6, TIs 0.5 for CDS and – FR 18, PRI 10, MI 0.4, TIs 0.7 for BFS. A high detection speckle reduction imaging (SRI HD) strength of 1 was used. The setting for the CrossXBeam technique was low, the CrossXBeam-type mean.

B-mode evaluation of the kidney in the longitudinal plane with a curved array was followed by documentation of vascularization: (1.) CDS images during systole with adapting of the color Doppler sensitivities from 15 to 5 cm/s; (2.) Identical BFS image during systole without altering the probe position or device setting; (3) Flow analysis of the interlobar and interlobular arteries in the lower, middle, and upper part of the transplant. The renal artery and vein were evaluated in the transverse plane. Thereafter, linear transducer images were obtained from the ventral part of the kidney (most proximal to the transducer) and assessed if available. 8 linear transducer sets were not completely obtainable or insufficient for analysis due to non-compliance. In total, 40 curved transducer and 32 linear transducer datasets were analyzed.

## Image analysis

The obtained datasets were analyzed in randomized order in consensus reading by two radiologists (J.H., 12 years of renal transplant ultrasound experience; E.D. 1 year of renal transplant ultrasound experience). Transplant vascularization was evaluated in four categories:

1. Delineation of the entire renal vascular tree (Grade 1 – clear demarcation of interlobar, together with arcuate and interlobular vessels; Grade 2 – clear demarcation of interlobar and cortical vessels, but no distinction of interlobular from arcuate vessels; Grade 3 – only clear demarcation of interlobar vessels, Grade 4 – insufficient demarcation; see ► **Fig. 1**);
2. Vessel density within the external cortex (interlobular vessels) in the ventral, dorsal, and lateral aspect of the kidney (Grade 1 – high density with close vessel alignment; Grade 2 – reduced vessel density with presence of small avascular gaps; Grade 3 – low vessel density with dominant large avascular gaps or absence of vessels; see ► **Fig. 2**) [20, 21].

3. Vessel-capsule distance (in cm); distance from the nearest visible cortical vessel to the renal capsule. Measurement from cutis to renal capsule (a) on CDS image with max. velocity range of 5 cm/s and from cutis to nearest vessel pixel on CDS (b) and on corresponding BFS image (b); vessel-capsule distance equals ((b)–(a)) [22, 23].
4. Cortical vessel count; number of distinguishable interlobular vessels in a length of 1 cm on corresponding CDS and BFS images (see ► **Fig. 3**). For standardization, measurement was performed perpendicular to the point where the vessel-capsule distance was assessed.
5. Linear transducer images were evaluated for categories 1–3, excluding the dorsal and lateral renal cortex as not depicted on the image.

## Statistical Analysis

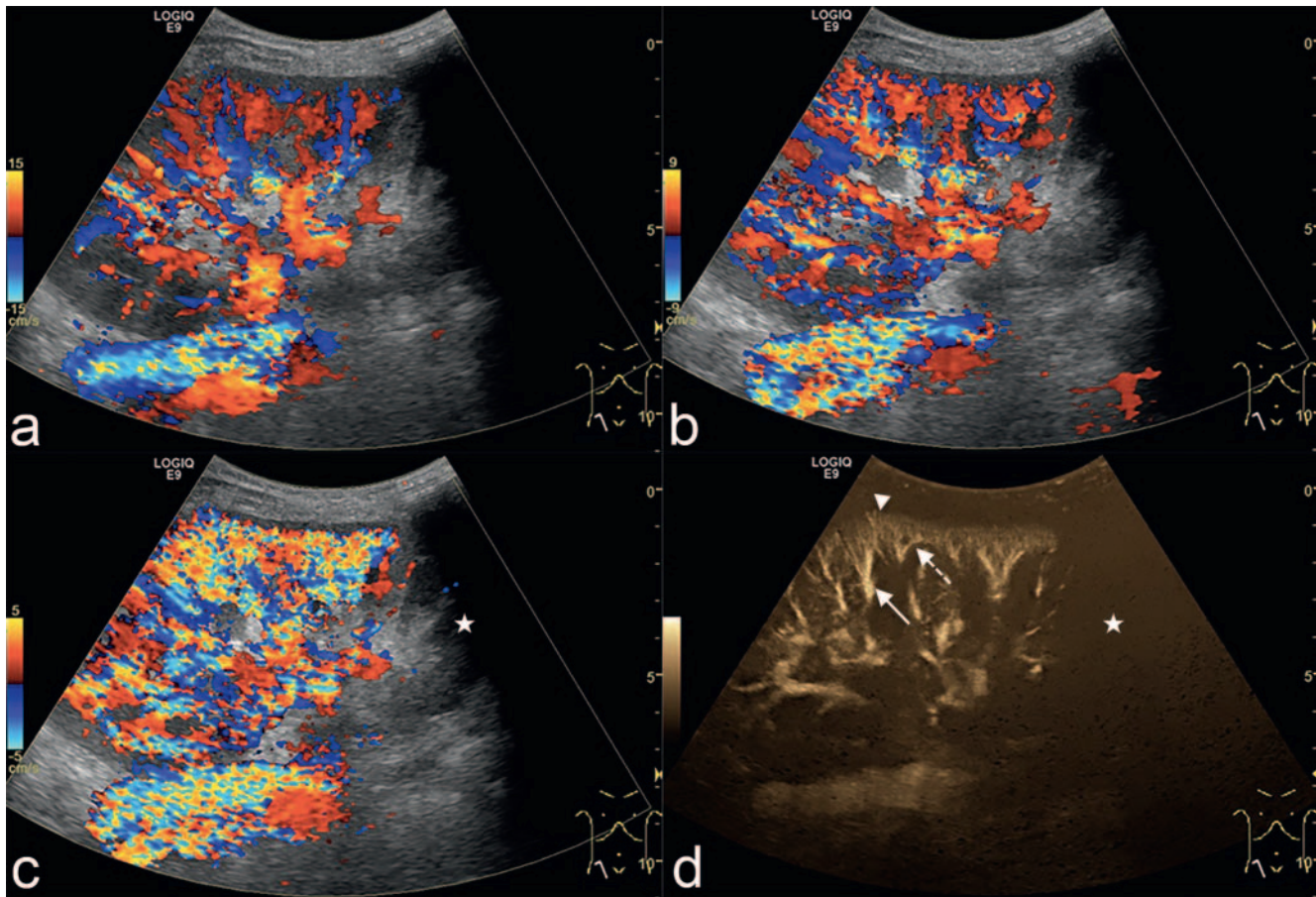
The corresponding datasets for CDS and BFS were compared using Fisher's exact tests for categorical variables (categories 1 and 2) and paired sample t-tests for numeric variables (categories 3 and 4). Normal distribution was tested for the numeric variables. If not stated otherwise, categorical variables are provided as numbers and percentages, continuous variables as mean ± standard deviation (SD). The effect of body mass index (BMI) and patient age (years) on the imaging results was calculated by ordinal regression (categories 1 and 2) and by a general linear model (categories 3 and 4). A P-value < 0.05 was considered statistically significant. All statistical analyses were computed with MedCalc for Windows (Mariakerke, Belgium), Excel (Microsoft Corporation, Redmond WA, USA), and SPSS (Version 24, IBM, Armonk, USA).

## RESULTS

### Curved transducer

Delineation of the entire renal vascular tree was superior with BFS compared with the velocity-optimized CDS images (grade 1.3 ± 0.66 vs. 2.48 ± 0.6,  $p < 0.001$ ) (► **Fig. 1, 4**). Also, vessel density and differentiability in the ventral external renal cortex was higher with BFS than with CDS (vessel density, grade 1.63 ± 0.59 vs. 2.05 ± 0.55,  $p = 0.01$ ; cortical vessel count, 8.05 ± 2.85 vessels vs. 5.65 ± 2.3 vessels,  $p < 0.001$ ; ► **Fig. 2–5**). The minimal vessel-capsule distance indicating the degree of vascularization of the peripheral cortex was lower with BFS compared with CDS (0.16 cm ± 0.13 cm vs. 0.31 cm ± 0.15 cm,  $p < 0.001$ ; ► **Fig. 5**). More distant from the transducer, in the dorsal and lateral aspect of the kidney graft, BFS was less sensitive than CDS (cortical vessel density, grade 2.65 ± 0.53 vs. 1.80 ± 0.61 and 2.64 ± 0.48 vs. 2 ± 0.64; each  $p < 0.001$ ; ► **Fig. 2, 4**). All data regarding the curved transducer are summarized in ► **Table 2**. The delineation of the renal vascular tree with CDS was superior in patients with a lower BMI ( $p = 0.04$ ). No significant effect of BMI or age on all other CDS parameters (vessel density, vessel-capsule distance, cortical vessel count) or on all BFS parameters was found.





► **Fig. 1** 7-year-old boy and corresponding ultrasound images of a kidney transplant in the longitudinal plane performed with a curved transducer using the CDS (**a–c**, max. velocity ranges 15 cm/s, 9 cm/s and 5 cm/s) and the BFS technique **d** are shown. Note the absence of vessels in the lower kidney due to an occluded accessory lower pole renal artery (**c**, **d**; asterisk). The upper and middle parts of the kidney are well vascularized. Lowering max. velocity ranges on CDS images **a–c** increases cortical vascular density but diminishes vessel delineation by aliasing and blurring artifacts. BFS **d** better depicts the entire vascular tree (interlobular vessel arrow, arcuate vessel dotted arrow, interlobular vessel arrowhead; renal vascular tree: grade 1) than CDS (**a–c**; renal vascular tree: grade 2). CDS has higher sensitivity for the detection of vessels in the deeper structures (cortical vessel density in the ventral aspect of the kidney: both grade 1; in the lateral aspect: CDS grade 1 and BFS grade 2; in the dorsal aspect: both grade 3). Technical parameters: a. Pulse repetition frequency (PRF) 1.4, b. PRF 0.8, c. PRF 0.5, a–c. Mechanical index (MI) 1.2, Thermal index in soft tissue (TIs) 0.9, Frequency (Frq) 3.6, Coded harmonic imaging (CHI) Frq 6.0, d. Pulse repetition interval (PRI) 12, MI 1.2, TIs 1.7. CDS = color Doppler sonography; BFS = B-flow sonography.

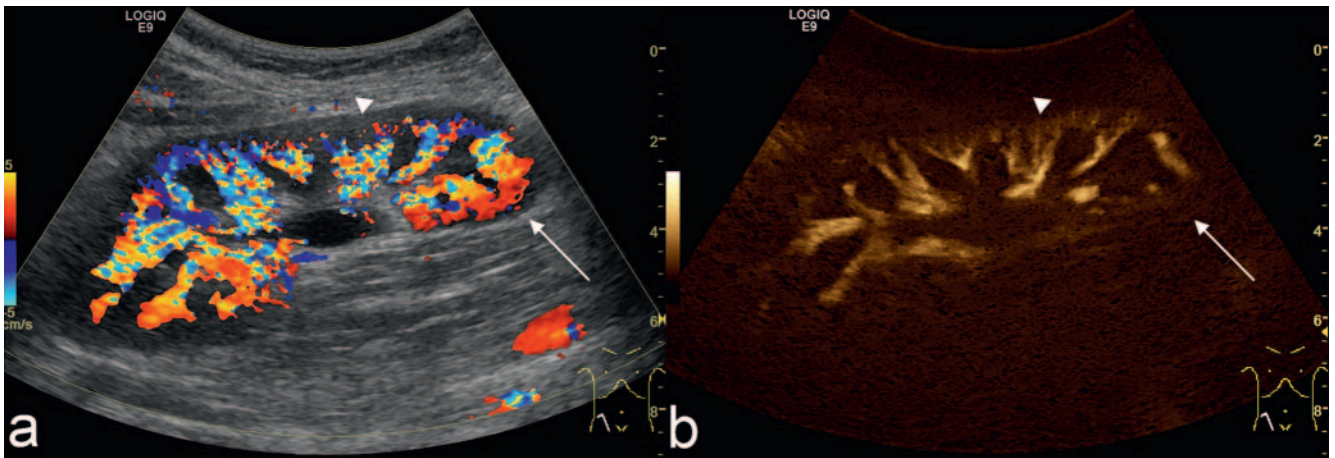
► **Abb. 1** 7-jähriger Junge und zugehörige Ultraschallbilder eines Nierentransplantats in Longitudinalschnitt mittels Sektorschallkopfes in CDS- (**a–c**, max. Geschwindigkeitsbereich 15 cm/s, 9 cm/s und 5 cm/s) und BFS-Technik **d**. Bemerke die Gefäßabwesenheit im kaudalen Nierenabschnitt aufgrund einer verschlossenen akzessorischen Unterpolararterie (**c**, **d**; Stern) Der kraniale und mittlere Nierenabschnitt zeigen sich regelrecht durchblutet. Das Herabsetzen der max. Geschwindigkeitsbereiche auf den CDS-Bildern **a–c** steigert die kortikale Gefäßdichte, schränkt die Gefäßdifferenzierbarkeit jedoch durch Aliasing und Unschärfeartefakte ein. BFS **d** stellt den gesamten Gefäßbaum besser dar (interlobäres Gefäß Pfeil, Bogengefäß gepunkteter Pfeil, interlobuläres Gefäß Pfeilkopf; renaler Gefäßbaum: Grad 1) als CDS (**a–c**; Grad 2). CDS hat eine höhere Sensitivität zur Gefäßdetektion in den tiefergelegenen Nierenabschnitten (Dichte der Kortexgefäße am ventral gelegenen Nierenanteil: beide Grad 1; lateral: CDS Grad 1, BFS Grad 2; dorsal: beide Grad 3). Technische Parameter: a Pulsrepetitionsfrequenz (PRF) 1,4, b PRF 0,8, c PRF 0,5, a–c mechanischer Index (MI) 1,2, thermischer Index in Weichteilen (TIs) 0,9, Frequenz (Frq) 3,6, Coded-harmonic-imaging (CHI) -Frq 6,0, d Pulsrepetitionsintervall (PRI) 12, MI 1,2, TIs 1,7. CDS = Color-Doppler-Sonografie; BFS = B-Flow-Sonografie

## Linear transducer

The analysis of the linear transducer images demonstrated no significant differences between CDS and BFS with respect to the delineation of the vascular tree, of the cortical vessels or the vessel-capsule distance (see ► **Fig. 6, 7**, ► **Table 3**).

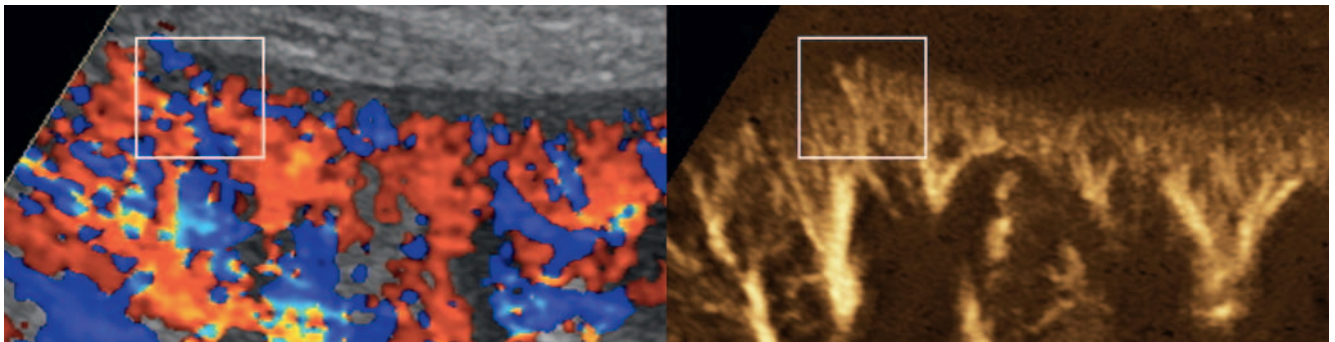
## Discussion

This study on kidney transplantation in children found that imaging of vascularization can be substantially improved by adding BFS as a non-Doppler-based vascular imaging technique to a standard protocol. The degree of transplant vascularization is a measure of transplant viability and impairment follows acute and chronic functional disorders [1, 4, 5].



► **Fig. 2** 10-year-old girl and corresponding ultrasound images with CDS (a, max. velocity range 5 cm/s) and BFS b of a kidney transplant positioned in the right flank. With CDS, large vascular-free gaps were noted in the ventral cortex (arrowhead; cortical vessel density grade 3), whereas the corresponding BFS image continuously depicts vessels in these areas (grade 1). Advantages of CDS can be seen in the dorsal and lateral part of the transplant with better detectability of vessels (arrow; cortical vessel density grade 1 and 1 with CDS and 3 and 3 with BFS). CDS = color Doppler sonography; BFS = B-flow sonography.

► **Abb. 2** 10-jähriges Mädchen und zugehörige Ultraschallbilder mit CDS (a, max. Geschwindigkeitsgrenze 5 cm/s) und BFS b eines in der rechten Flanke positionierten Nierentransplantats. Mit CDS zeigen sich große avaskuläre Lücken im ventralen Kortex (Pfeilkopf; kortikale Gefäßdichte Grad 3), während das korrespondierende BFS-Bild eine kontinuierliche Gefäßanreihung in diesen Abschnitten darstellt (Grad 1). Vorteile von CDS erkennt man im dorsalen und lateralen Transplantatabschnitt mit besserer Gefäßnachweisbarkeit (Pfeil; kortikale Gefäßdichte Grad 1 bzw. 1 mit CDS und 3 bzw. 3 mit BFS). CDS = Color-Doppler-Sonografie; BFS = B-Flow-Sonografie.

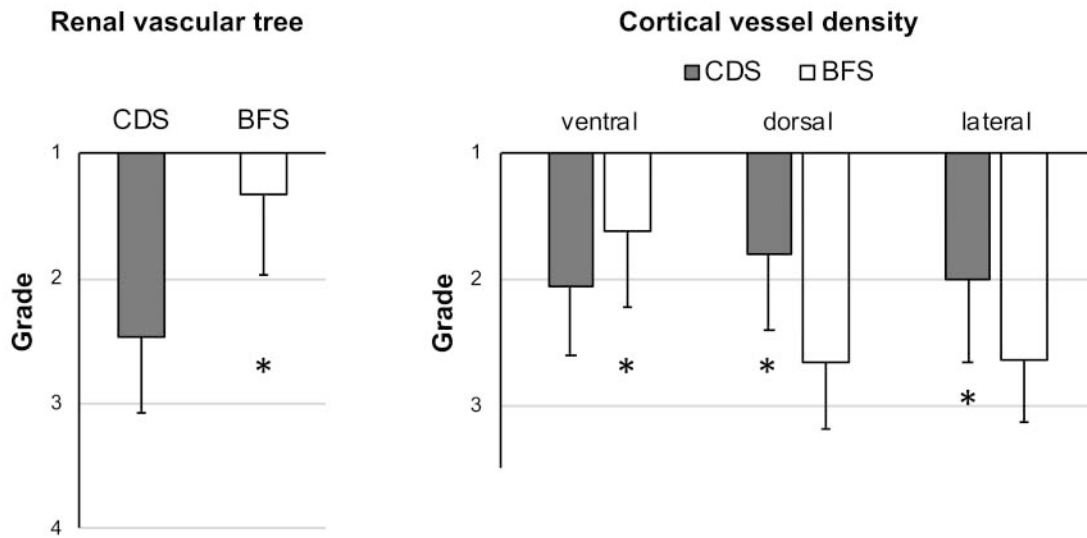


► **Fig. 3** Detail magnification of the renal cortex in a 7-year-old patient after kidney transplantation (same patient as in Fig. 1) to illustrate vessel count performed in a region of interest with a length of 1 cm (box). On CDS (left image) the interlobular vessels are masked by aliasing and single vessels can only be identified by an opposing flow direction (max. vessel count: 7). The higher spatial resolution of BFS allows clearer separation of neighboring cortical vessels (max. vessel count: 12).

► **Abb. 3** Detailvergrößerung des Nierenkortex bei einem 7-jährigen Patienten nach Nierentransplantation (gleicher Patient aus Abb. 1). Auf einer Strecke von 1 cm (Kasten) erfolgte die Auszählung differenzierbarer Kortexgefäße. Mit CDS (linkes Bild) werden einzelne Interlobulärgefäße durch Aliasing maskiert und sind nur durch entgegengesetzte Flussrichtungen zu differenzieren (max. 7 Gefäße). Die höhere räumliche Auflösung von BFS erlaubt eine deutlichere Separation benachbarter Kortexgefäße (max. 12 Gefäße).

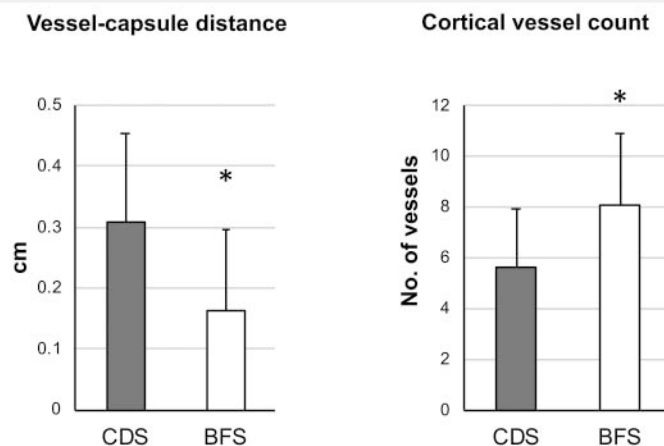
As the quality of vessel delineation also depends on the applied ultrasound technique, these methodical aspects have to be carefully controlled [20, 23–26]. In a preliminary study with renal transplantation in adults, Russo et al. showed that BFS compared with Doppler-based techniques can depict the cortical vasculature more clearly and thus characterize causes of vascular complications more precisely [16]. Further studies have to be performed in children to test clinical meaningfulness and capability to monitor transplant viability.

The advantages of BFS can be attributed to the inherent properties of B-mode imaging. Based on subtraction of B-mode images, flow images with high spatial and temporal resolution can be generated [11]. In comparison with CDS, BFS was substantially better for the delineation of the entire renal vascular tree allowing a more detailed depiction of the cortical vascular architecture together with the feeding segmental arteries on a single preset. In our clinic, we use the high spatial resolution of BFS for subsequent exact and quick placement of spectral Doppler volumes. BFS



► **Fig. 4** Grading of the renal vascular tree and cortical vessel density within the ventral, dorsal and lateral aspect of the kidney transplant on curved array images. Data are mean values and standard deviations. CDS = color Doppler sonography; BFS = B-flow sonography. Renal vascular tree: Grade 1 – clear demarcation of all vessels; Grade 2 – clear demarcation of interlobar from cortical vessels, no distinction of interlobular from arcuate vessels; Grade 3 – just clear demarcation of interlobar vessels, Grade 4 – insufficient demarcation. Cortical vessel density: Grade 1 – high vessel density with close alignment; Grade 2 – reduction of vessel density with avascular gaps; Grade 3 – large intervals without vascularity or absence of cortical vessels. \*Statistically significant.

► **Abb. 4** Evaluation des renalen Gefäßbaums und der kortikalen Gefäßdichte im ventralen, dorsalen und lateralen Nierentransplantatabschnitt auf Sektorschallkopfbildern. Die Daten sind angegeben als Mittelwert und Standardabweichung. CDS = Color-Doppler-Sonografie; BFS = B-Flow-Sonografie. Renal vascular tree (renaler Gefäßbaum): Grad 1 – eindeutige Abgrenzbarkeit der gesamten Gefäße; Grad 2 – eindeutige Abgrenzbarkeit von Interlobär- und Kortextgefäßen, ohne Differenzierbarkeit zwischen Interlobulär- und Arcuataegefäß; Grad 3 – lediglich gute Abgrenzbarkeit der Interlobärgefäße; Grad 4 – insuffiziente Differenzierbarkeit. Cortical vessel density (Dichte der Kortextgefäße): Grad 1 – hohe Gefäßdichte mit enger Aneinanderreihung; Grad 2 – reduzierte Gefäßdichte mit avaskulären Lücken; Grad 3 – große avaskuläre Intervalle oder Fehlen kortikaler Gefäße. \*statistisch signifikant.

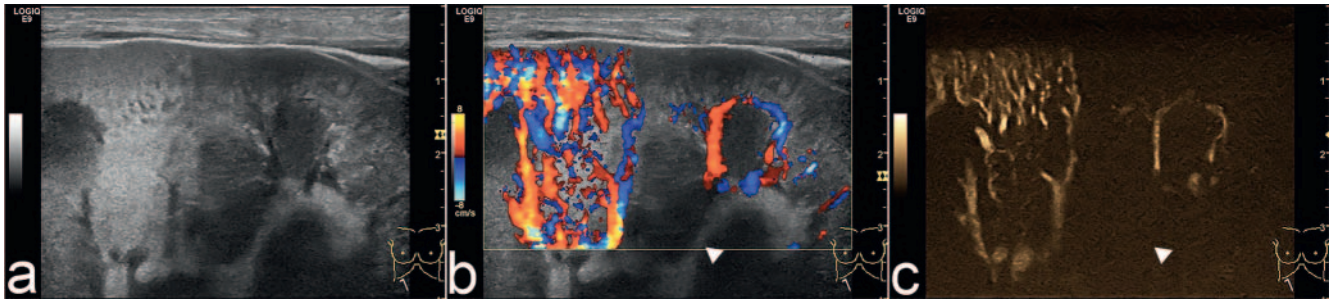


► **Fig. 5** Assessment of vessel-capsule distance and the best cortical vessel count comparing BFS and CDS within the ventral cortex of the kidney transplant on curved array images. Data are mean values and standard deviations. CDS = color Doppler sonography; BFS = B-flow sonography. Vessel-capsule distance: distance from the most external vessel to the renal capsule in cm. Cortical vessel count: Best cortical vessel count in the ventral renal cortex with a length of 1 cm. \*Statistically significant.

► **Abb. 5** Evaluation des Gefäß-Kapsel-Abstands und der besten kortikalen Gefäßauszählung im ventralen Nierenkortex auf Sektorschallkopfbildern verglichen zwischen BFS und CDS. Die Daten sind angegeben als Mittelwert und Standardabweichung. CDS = Color-Doppler-Sonografie; BFS = B-Flow-Sonografie. Vessel-capsule distance (Gefäß-Kapsel-Abstand): Abstand des externsten kortikalen Gefäßes zur Nierenkapsel in cm. Cortical vessel count (kortikale Gefäßzählung): maximale Anzahl kortikaler Gefäße auf 1 cm.

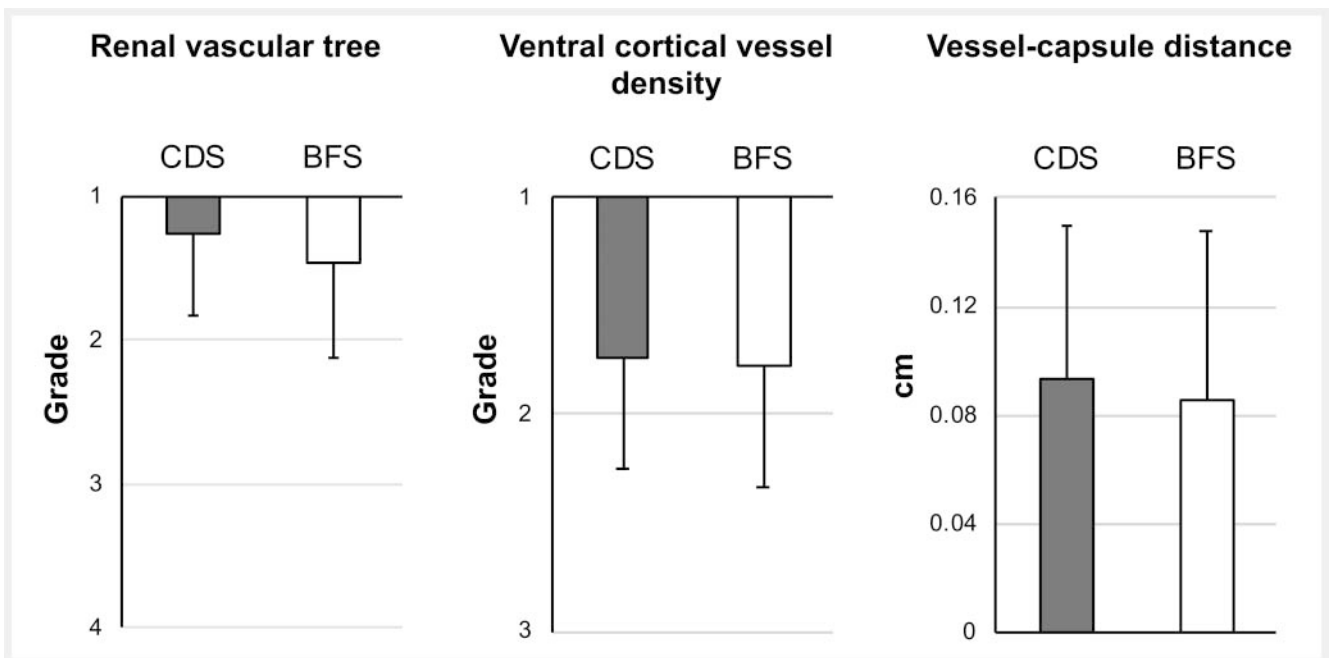
This document was downloaded for personal use only. Unauthorized distribution is strictly prohibited.





► **Fig. 6** 7-year-old boy (same as in Fig. 1, 3) with kidney transplant positioned in the right flank. Corresponding ultrasound images in the longitudinal plane with a linear transducer using the B-mode **a**, the CDS **b**, and the BFS technique **c** are shown. Nearly complete absence of cortical vessels in the right lower part of the cortex is shown due to occlusion of an accessory renal artery (arrowheads). The upper left part of the cortex has good vascularization, equally shown in the CDS and the BFS technique. CDS = color Doppler sonography; BFS = B-flow sonography.

► **Abb. 6** 7-jähriger Junge (derselbe wie in Abb. 1, 3) mit in der rechten Flanke positioniertem Nierentransplantat. Korrespondierende Ultraschallbilder in Longitudinalschnitt unter Verwendung eines Linearschallkopfes in B-Mode - **a**, CDS- **b** und BFS-Technik **c**. Nahezu vollständiges Fehlen von Kortextgefäßen im rechten, kaudalen Kortex aufgrund einer verschlossenen akessorischen Unterpolarterie (Pfeilköpfe). Der kraniale, linke Abschnitt ist regelrecht perfundiert, ebenso gut mit CDS wie mit BFS dargestellt. CDS = Color-Doppler-Sonografie; BFS = B-Flow-Sonografie.



► **Fig. 7** Assessment of vascularity comparing BFS and CDS when applying a linear transducer. No statistical significance was found. Data are mean values and standard deviations. CDS = color Doppler sonography; BFS = B-flow sonography. Renal vascular tree: Grade 1 – clear demarcation of all vessels; Grade 2 – clear demarcation of interlobar from cortical vessels, no distinction of interlobular from arcuate vessels; Grade 3 – just clear demarcation of interlobar vessels, Grade 4 – insufficient differentiability. Cortical vessel density: Grade 1 – high vessel density with close alignment; Grade 2 – reduction of vessel density with avascular gaps; Grade 3 – large intervals without vascularity or absence of cortical vessels. Vessel-capsule distance: distance from the most external vessel to the renal capsule in cm.

► **Abb. 7** Evaluation der renalen Gefäßversorgung mit BFS verglichen mit CDS bei der Verwendung eines Linearschallkopfes. Wir fanden keine statistische Signifikanz. Die Daten sind angegeben als Mittelwert und Standardabweichung. CDS = Color-Doppler-Sonografie; BFS = B-Flow-Sonografie. Renal vascular tree (renaler Gefäßbaum): Grad 1 – eindeutige Abgrenzbarkeit der gesamten Gefäße; Grad 2 – eindeutige Abgrenzbarkeit von Interlobär- und Kortextgefäßen, ohne Differenzierbarkeit zwischen Interlobulär- und Arcuataefäßen; Grad 3 – lediglich gute Abgrenzbarkeit der Interlobärgefäße; Grad 4 – insuffiziente Differenzierbarkeit. Cortical vessel density (Dichte der Kortextgefäße): Grad 1 – hohe Gefäßdichte mit enger Aneinanderreihung; Grad 2 – reduzierte Gefäßdichte mit avaskulären Lücken; Grad 3 – große avaskuläre Intervalle oder Fehlen kortikaler Gefäße. Vessel-capsule distance (Gefäß-Kapsel-Abstand): Abstand des externsten kortikalen Gefäßes zur Nierenkapsel in cm. \* statistisch signifikant

► **Table 2** Comparison of vessel delineation in kidney transplants with the BFS and the CDS technique using a curved transducer.

► **Tab. 2** Vergleich der Gefäßdarstellung in Nierentransplantaten mit BFS- und CDS-Technik unter Verwendung eines Sektorschallkopfes.

parameter	BFS	CDS	p-value
renal vascular tree (grades 1–4)	1.33 ± 0.66	2.48 ± 0.6	<0.001
cortical vessel density (grades 1–3)			
▪ ventral external cortex	1.63 ± 0.59	2.05 ± 0.55	0.01
▪ dorsal external cortex	2.65 ± 0.53	1.80 ± 0.61	<0.001
▪ lateral external cortex	2.64 ± 0.48	2 ± 0.64	<0.001
vessel-capsule distance (cm)	0.16 ± 0.13	0.31 ± 0.15	<0.001
cortical vessel count (no.)	8.05 ± 2.85	5.65 ± 2.30	<0.001

Data are mean values and standard deviations. CDS = color Doppler sonography; BFS = B-flow sonography. Renal vascular tree: Grade 1 – clear demarcation of all vessels; Grade 2 – clear demarcation of interlobar from cortical vessels, no distinction of interlobular from arcuate vessels; Grade 3 – just clear demarcation of interlobar vessels, Grade 4 – insufficient differentiability. Cortical vessel density: Grade 1 – high vessel density with close alignment; Grade 2 – reduction of vessel density with avascular gaps; Grade 3 – large intervals without vascularity or absence of cortical vessels. Vessel-capsule distance: distance from the most external vessel to the renal capsule in cm. Cortical vessel count: Best cortical vessel count in the external renal cortex with a length of 1 cm.

Daten angegeben als Mittelwerte mit Standardabweichung. CDS = Color-Doppler-Sonografie; BFS = B-Flow-Sonografie. Renal vascular tree (renaler Gefäßbaum): Grad 1 – eindeutige Abgrenzbarkeit der gesamten Gefäße; Grad 2 – eindeutige Abgrenzbarkeit von Interlobär- und Kortexgefäßen, ohne Differenzierbarkeit zwischen Interlobulär- und Arcuataegefäßen; Grad 3 – lediglich gute Abgrenzbarkeit der Interlobärgefäße; Grad 4 – insuffiziente Abgrenzbarkeit. Cortical vessel density (Dichte der Kortexgefäße): Grad 1 – hohe Gefäßdichte mit enger Aneinanderreihung; Grad 2 – reduzierte Gefäßdichte mit avaskulären Lücken; Grad 3 – große avaskuläre Intervalle oder Fehlen kortikaler Gefäße. Vessel-capsule distance (Gefäß-Kapsel-Abstand): Abstand des externsten kortikalen Gefäßes zur Nierenkapsel in cm. Cortical vessel count (kortikale Gefäßzählung): maximale Anzahl kortikaler Gefäße auf 1 cm.

► **Table 3** Comparison of vessel delineation in kidney transplants with the BFS and the CDS technique using a linear transducer.

► **Tab. 3** Vergleich der Gefäßdarstellung in Nierentransplantaten mit BFS- und CDS-Technik unter Verwendung eines Linearschallkopfes.

parameter	BFS	CDS	p-value
renal vascular tree (grades 1–4)	1.45 ± 0.68	1.26 ± 0.58	0.31
cortical vessel density in the ventral external cortex (grades 1–3)	1.77 ± 0.56	1.74 ± 0.52	0.92
vessel-capsule distance (cm)	0.09 ± 0.06	0.09 ± 0.05	0.61

Data are mean values and standard deviations. CDS = color Doppler sonography; BFS = B-flow sonography. Renal vascular tree: Grade 1 – clear demarcation of all vessels; Grade 2 – clear demarcation of interlobar from cortical vessels, no distinction of interlobular from arcuate vessels; Grade 3 – just clear demarcation of interlobar vessels, Grade 4 – insufficient differentiability. Cortical vessel density: Grade 1 – high vessel density with close alignment; Grade 2 – reduction of vessel density with avascular gaps; Grade 3 – large intervals without vascularity or absence of cortical vessels. Vessel-capsule distance: distance from the most external vessel to the renal capsule in cm.

Daten angegeben als Mittelwerte mit Standardabweichung. CDS = Color-Doppler-Sonografie; BFS = B-Flow-Sonografie. Renal vascular tree (renaler Gefäßbaum): Grad 1 – eindeutige Abgrenzbarkeit der gesamten Gefäße; Grad 2 – eindeutige Abgrenzbarkeit von Interlobär- und Kortexgefäßen, ohne Differenzierbarkeit zwischen Interlobulär- und Arcuataegefäßen; Grad 3 – lediglich gute Abgrenzbarkeit der Interlobärgefäße; Grad 4 – insuffiziente Abgrenzbarkeit. Cortical vessel density (Dichte der Kortexgefäße): Grad 1 – hohe Gefäßdichte mit enger Aneinanderreihung; Grad 2 – reduzierte Gefäßdichte mit avaskulären Lücken; Grad 3 – große avaskuläre Intervalle oder Fehlen kortikaler Gefäße. Vessel-capsule distance (Gefäß-Kapsel-Abstand): Abstand des externsten kortikalen Gefäßes zur Nierenkapsel in cm.

shows a dynamic range to capture fast-flow and low-flow vessels on a single flow image, as initially observed by Wachsberg et al. [12]. In contrast, realistic visualization of the renal vasculature is technically more demanding and time-consuming with CDS, where velocity encoding sensitivities need to be adapted to the

region of interest with different settings for sensitive detection of low-flow cortical vessels or fast-flow feeding arteries to avoid aliasing artifacts [2, 12]. We showed that BFS can separate the densely packed interlobular and arcuate vessels of the external

renal cortex, whereas in CDS blurring boundaries of neighboring vessels were noted and explained by blooming artifacts.

On the other hand, BFS is prone to sound beam attenuation, which increases with depth [10]. Applying B-flow on kidney grafts in children is favorable as the organ is situated close to the skin in the iliac fossa with little adjacent subcutaneous fat [2]. Yet, also in our pediatric cohort, BFS was less sensitive than color Doppler for vessel depiction in the deeper areas more distant from the center of the transducer. Additionally, we did not notice significant differences between CDS and the BFS grading of transplant vascularity when using a linear, high-resolution transducer. As CDS in overlay mode also carries information about structural parenchymal integrity, e. g. can detect cortical scarring, we favor CDS for this application. However, due to their lower display range, linear transducers are limited to assessment of accessible regions of the transplant, e. g. the superficial part of the lower pole.

There are further methods recently introduced by different manufacturers that seem advantageous for the sonographic depiction of complex flow and small vessels, such as Advanced Dynamic Flow (ADF) or superb micro-vascular imaging (SMI) [27, 28]. However, a common problem of these newer techniques, as well as of BFS, is the lacking overall availability on the ultrasound systems. Also, contrast-enhanced ultrasound (CEUS) is an increasingly used method for vascular assessment in kidney transplantation in adults and has been recommended for this use by the European federation of Societies in Ultrasound in Medicine and Biology (EFSUMB) [24, 30, 31]. To our knowledge, CEUS has not yet been systematically applied in pediatric kidney transplantation as its intravascular application in children is only approved for the characterization of focal liver lesions so far [29].

Our study has the following limitations: (1) The study design is retrospective and is therefore dependent on medical documentation and principally prone to selection bias. (2) Results of ultrasound investigations are operator-dependent and require a high level of skill. To guarantee a high level of data consistency, the included data points were limited to examinations performed by a single expert pediatric radiologist. The inter- and intra-operator variability of BFS and CDS cannot be reported (3). The number of patients in our study was relatively low and heterogeneous with regard to age, days after transplantation, BMI, transplantation type (living or cadaveric), clinical and laboratory findings (► **Table 1**).

In summary, BFS yields better results than CDS for assessing the overall vascularity in pediatric kidney transplantation and thereby could improve monitoring of transplant viability. As suggested by previous studies focusing on other vascular territories, the B-flow technique may be especially useful in infants and young children [18, 19]. BFS is less favorable in larger patients and for the deeper parts of the kidney due to sound beam attenuation and should thereby be used in addition to Doppler-based ultrasound techniques. Further standardization of the ultrasound protocols and the reporting of the results in pediatric kidney transplantation is desirable for the future. There are other fields of diagnostic ultrasound, e. g. in the domain of screening and surveillance where standardization is already more advanced [32].

## CLINICAL RELEVANCE OF THE STUDY

- Additional monitoring with BFS improves monitoring of kidney transplant viability.
- Acute and chronic functional disorders impair transplant vascularity. A higher quality of vessel delineation may facilitate the early detection of graft damage.
- Adding BFS to a standard protocol after kidney transplantation accelerates workflow as an accurate overview of the global vascular tree is obtained and subsequent detailed vascular assessment can be performed, e. g. placement of spectral doppler volumes.

## Conflict of Interest

The authors declare that they have no conflict of interest.

## References

- [1] Burgos FJ, Pascual J, Marcen R et al. The role of imaging techniques in renal transplantation. *World J Urol* 2004; 22: 399–404. doi:10.1007/s00345-004-0412-1
- [2] Baxter GM. Imaging in renal transplantation. *Ultrasound Q* 2003; 19: 123–138
- [3] Sugi MD, Joshi G, Maddu KK et al. Imaging of Renal Transplant Complications throughout the Life of the Allograft: Comprehensive Multimodality Review. *Radiographics* 2019; 39: 1327–1355. doi:10.1148/rq.2019190096
- [4] Irshad A, Ackerman SJ, Campbell AS et al. An overview of renal transplantation: current practice and use of ultrasound. *Semin Ultrasound CT MR* 2009; 30: 298–314
- [5] Nixon JN, Biyyam DR, Stanescu L et al. Imaging of pediatric renal transplants and their complications: a pictorial review. *Radiographics* 2013; 33: 1227–1251. doi:10.1148/rg.335125150
- [6] Grenier N, Douws C, Morel D et al. Detection of vascular complications in renal allografts with color Doppler flow imaging. *Radiology* 1991; 178: 217–223. doi:10.1148/radiology.178.1.1984307
- [7] Taylor KJ, Morse SS, Rigsby CM et al. Vascular complications in renal allografts: detection with duplex Doppler US. *Radiology* 1987; 162: 31–38. doi:10.1148/radiology.162.1.3538150
- [8] Platt JF, Rubin JM, Ellis JH. Acute renal obstruction: evaluation with intrarenal duplex Doppler and conventional US. *Radiology* 1993; 186: 685–688. doi:10.1148/radiology.186.3.8430174
- [9] Barba J, Rioja J, Robles JE et al. Immediate renal Doppler ultrasonography findings (<24h) and its association with graft survival. *World J Urol* 2011; 29: 547–553. doi:10.1007/s00345-011-0666-3
- [10] Weskott HP. B-flow – a new method for detecting blood flow. *Ultraschall in Med* 2000; 21: 59–65. doi:10.1055/s-2000-319
- [11] Henri P, Tranquart F. B-flow ultrasonographic imaging of circulating blood. *J Radiol* 2000; 81: 465–467
- [12] Wachsberg RH. B-flow, a non-Doppler technology for flow mapping: early experience in the abdomen. *Ultrasound Q* 2003; 19: 114–122
- [13] Mikami T, Takahashi A, Houkin K. Evaluation of blood flow in carotid artery stenosis using B-flow sonography. *Neurol Med Chir (Tokyo)* 2003; 43: 528–532; discussion 533

- [14] Hancerliogullari KO, Soyer T, Tosun A et al. Is B-Flow USG superior to Color Doppler USG for evaluating blood flow patterns in ovarian torsion? *J Pediatr Surg* 2015; 50: 1156–1161. doi:10.1016/j.jpedsurg.2014.08.028
- [15] Wachsberg RH. B-flow imaging of the hepatic vasculature: correlation with color Doppler sonography. *Am J Roentgenol* 2007; 188: W522–W533. doi:10.2214/Am J Roentgenol.06.1161
- [16] Russo E, Cerbone V, Sciano D et al. Posttransplant renal monitoring with B-flow ultrasonography. *Transplant Proc* 2010; 42: 1127–1129. doi:10.1016/j.transproceed.2010.03.050
- [17] Hongmei W, Ying Z, Ailu C et al. Novel application of four-dimensional sonography with B-flow imaging and spatiotemporal image correlation in the assessment of fetal congenital heart defects. *Echocardiography* 2012; 29: 614–619. doi:10.1111/j.1540-8175.2011.01639.x
- [18] Groth M, Dammann E, Arndt F et al. Comparison of B-Mode with B-Flow Sonography for the Evaluation of Femoral Arteries in Infants. *Rofo* 2017. doi:10.1055/s-0043-112249
- [19] Groth M, Ernst M, Deindl P et al. B-Flow Sonography for Evaluation of Basal Cerebral Arteries in Newborns. *Clin Neuroradiol* 2019; 29: 95–100. doi:10.1007/s00062-017-0624-6
- [20] Trillaud H, Merville P, Tran Le Linh P et al. Color Doppler sonography in early renal transplantation follow-up: resistive index measurements versus power Doppler sonography. *Am J Roentgenol* 1998; 171: 1611–1615. doi:10.2214/ajr.171.6.9843297
- [21] Martinoli C, Crespi G, Bertolotto M et al. Interlobular vasculature in renal transplants: a power Doppler US study with MR correlation. *Radiology* 1996; 200: 111–117. doi:10.1148/radiology.200.1.8657897
- [22] Gruenewald S, Skerrett D, Dolimier D et al. Technique of color Doppler quantification of vascularity in transplanted kidneys. *J Clin Ultrasound* 2002; 30: 151–157
- [23] Nankivell BJ, Chapman JR, Gruenewald SM. Detection of chronic allograft nephropathy by quantitative doppler imaging. *Transplantation* 2002; 74: 90–96
- [24] Schwenger V, Korosoglou G, Hinkel UP et al. Real-time contrast-enhanced sonography of renal transplant recipients predicts chronic allograft nephropathy. *Am J Transplant* 2006; 6: 609–615. doi:10.1111/j.1600-6143.2005.01224.x
- [25] Radermacher J, Mengel M, Ellis S et al. The renal arterial resistance index and renal allograft survival. *N Engl J Med* 2003; 349: 115–124. doi:10.1056/NEJMoa022602
- [26] Fischer T, Filimonow S, Dieckhofer J et al. Improved diagnosis of early kidney allograft dysfunction by ultrasound with echo enhancer—a new method for the diagnosis of renal perfusion. *Nephrol Dial Transplant* 2006; 21: 2921–2929. doi:10.1093/ndt/gfl313
- [27] Heling KS, Chaoui R, Bollmann R. Advanced dynamic flow – a new method of vascular imaging in prenatal medicine. A pilot study of its applicability. *Ultraschall in Med* 2004; 25: 280–284. doi:10.1055/s-2004-813383
- [28] Machado P, Segal S, Lyshchik A et al. A Novel Microvascular Flow Technique: Initial Results in Thyroids. *Ultrasound Q* 2016; 32: 67–74. doi:10.1097/RUQ.000000000000156
- [29] Sidhu PS, Cantisani V, Deganello A et al. Role of Contrast-Enhanced Ultrasound (CEUS) in Paediatric Practice: An EFSUMB Position Statement. *Ultraschall in Med* 2017; 38: 33–43. doi:10.1055/s-0042-110394
- [30] Harvey CJ, Sidhu PS, Bachmann Nielsen M. Contrast-enhanced ultrasound in renal transplants: applications and future directions. *Ultraschall in Med* 2013; 34: 319–321. doi:10.1055/s-0033-1350138
- [31] Sidhu PS, Cantisani V, Dietrich CF et al. The EFSUMB Guidelines and Recommendations for the Clinical Practice of Contrast-Enhanced Ultrasound (CEUS) in Non-Hepatic Applications: Update 2017 (Long Version). *Ultraschall in Med* 2018; 39: e2–e44. doi:10.1055/a-0586-1107
- [32] Morgan TA, Maturen KE, Dahiya N et al. US LI-RADS: ultrasound liver imaging reporting and data system for screening and surveillance of hepatocellular carcinoma. *Abdom Radiol (NY)* 2018; 43: 41–55. doi:10.1007/s00261-017-1317-y